Model-Based Approach for Magnetic Reconstruction in Axisymmetric Nuclear Fusion Machines

Angelo Cenedese, *Member, IEEE*, Paolo Bettini, and Matteo Bonotto

***Abstract*— This paper describes an approach for the magnetic reconstruction of large-scale tokamak devices that is suitable for real-time employment in order to provide reference for active control action during the whole plasma evolution. This problem can be seen as a *free boundary problem*, where the shape features of the plasma are determined by the equilibrium with the external sources, namely, the active circuit currents and the eddy currents flowing in the passive structures. In this respect, a dynamic model is needed to estimate the induced currents and provide a consistent representation of the whole system behavior during the entire plasma discharge. Such a model is then coupled with an iterative optimization procedure to provide a model of the plasma that, superimposed with the external sources, minimizes the error of the reconstructed magnetic map with reference to the available sensor measurements. The analysis and validation of this approach are presented, resulting in a procedure that appears to accurately follow the behavior of the system during both slow varying evolution and strongly dynamic events.**

***Index Terms*— Plasma model, real-time control, reconstruction code, tokamak.**

I. Introduction

TOKAMAKS are fusion devices that envisage a scenario operation starting from a ramp-up phase (RU) of the plasma current from zero up to several Mega-ampere (MA), developing through a main flat-top phase (FT) of *stable* equilibrium, and terminating through a ramp-down phase (RD); moreover, the current generation of tokamaks are experimenting highly elongated plasmas for the future reactor employment for optimized performance [1], [2]. Both these aspects call for the employment of active control systems to ensure safety and efficiency, in both the feedforward component to govern the discharge evolution and in the feedback component to counteract noise, disturbances, and unmodeled dynamics [3].

To this aim, reconstruction of the plasma shape and position to support both the design and exploitation of control loops appears as a *free boundary problem*, which can be solved through numerical codes developed for full MHD equilibrium reconstruction (see [4]), or approximated through more agile model-based schemes particularly suitable for real-time use [5]. In this context, and given the scenario evolution above, the role of dynamical modeling appears of paramount importance during the regime transitions and when considering the disturbances that may affect the plasma, which excite the coupled subsystems such as the plasma itself, the electromagnetic circuits, and the passive conducting structures [6]. An effort in this sense is given in [7], where offline assessment of electromagnetic loads on the surface of the ITER plasma-facing components is obtained through integration of 2-D and 3-D numerical codes; this allows to reconstruct the pattern of induced currents basing on a measurement fitting procedure. More recently, a dynamic filamentary model for the plasma has been proposed, in combination with a low-order finite element (FE) model of the conducting structures, which allows the representation of an advanced plasma configuration and scenario transitions, still relying on a measurement optimization approach [8].

Similar to the approach presented in [8], in this paper also, identification of eddy current patterns in the passive structure is discussed and a complete model that accounts for the plasma–structure interactions is proposed, to allow a consistent reconstruction of the plasma shape on the poloidal cross section of the machine during dynamic events and throughout the discharge evolution. In this respect, and differently from [7], the contribution here is aimed for use as an observer within a real-time control loop and not only as an optimization tool for the design.

The remainder of this paper is as follows. Section II provides an overview of the approach adopted in the proposed procedure, and describes the models employed by structuring the algorithm in a modular fashion. Section III gives a validation of the code, referring to a full plasma scenario evolution designed for ITER operation; finally, in Section IV some conclusions are drawn, together with an outline of the possible further developments and research avenues.

II. Modeling Approach and Modules

A. Notation

In this paper, the scalar parameters and variables are denoted by nonbold uppercase or lowercase letters, while the vector

Manuscript received June 17, 2016; revised November 3, 2017; accepted January 14, 2018. Date of publication February 5, 2018; date of current version March 8, 2018. This work was supported by the University of Padua under Grant CPDA144817. The review of this paper was arranged by Senior Editor S. J. Gitomer. *(Corresponding author: Angelo Cenedese.)*

A. Cenedese is with the Department of Information Engineering, University of Padua, 35122 Padua, Italy (e-mail: angelo.cenedese@unipd.it).

P. Bettini and M. Bonotto are with the Department of Industrial Engineering, University of Padua, 35122 Padua, Italy, and also with the Center of Research on Fusion, University of Padua, 35122 Padua, Italy.

Color versions of one or more of the figures in this paper are available online at http://ieeexplore.ieee.org.

Digital Object Identifier 10.1109/TPS.2018.2796504

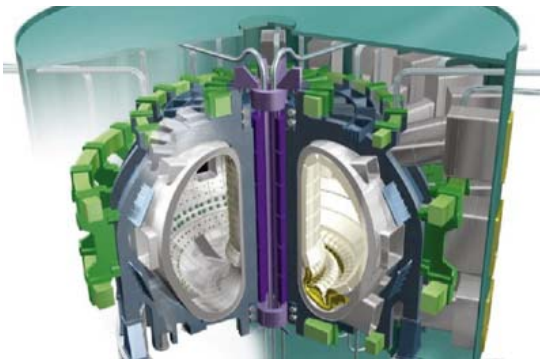

Fig. 1. Schematic of the ITER machine: the active circuits are shown in green (PF–VS) and violet (CS), while the passive structures are shown in light gray. Image provided courtesy of Fusion for Energy.

and matrix quantities are denoted, respectively, by bold lowercase and bold uppercase symbols.

B. Overview and Rationale

The algorithm for magnetic reconstruction is based on a model of the machine structure that includes both the active magnetic systems and the metallic passive structures: with reference to the specific application to an ITER-like machine (see Fig. 1), this model considers the active coils [central solenoid (CS), poloidal field coils (PF), and vertical stabilization coils (VS)], and the passive structures (inner and outer vessels, and vertical and triangular supports). This information is encoded into a set of resistance and inductance matrices that describe the interactions among the conductive components and a set of Green's functions that describe the interactions among these conductors and the surrounding space. Hence, the proposed code takes the signals coming from the magnetic sensors as the input, and provides the boundary location as a set of gap distances as the output, together with flux information at specified points on the poloidal plane $\Pi(r, z)$.

The code is structured into four main cascading modules (see Fig. 2) and takes the active coil currents $\mathbf{i_s}$ and the magnetic measurements $\mathbf{m}$ as the input for the whole procedure: its core is the approximation of the plasma with an equivalent filamentary model that is first roughly identified (currents $\mathbf{i}_{e0}$) to allow modeling of the passive structure dynamics (i.e., eddy currents $\mathbf{i}_c$) and then refined iteratively (currents $\mathbf{i}_e$) so as to describe a wide variety of plasma current distributions, from the peaked ones, to the pedestal current ones. The output of the algorithm is the plasma model $\mathbf{i}_e$ in addition to the shape parameters γ, in terms of plasma-firstwall distances (gaps) or other integral figures (e.g., elongation, triangularity).

C. First Approximation Plasma Modeling

Magnetic measurements outside the plasma have traditionally been a simple and reliable method for finding the plasma configuration in fusion experiments. This is related to the ith order moment of the plasma current distribution q_i through the integral calculation [9]

$$q_i = \int_\Omega \chi_i \cdot j_\phi d\Omega = \oint_{\partial\Omega} (\chi_i B_t + \xi_i B_n) d\ell \quad i = 1, 2, \ldots \tag{1}$$

where $\Omega \subset \Pi$ is the plasma cross section and $\partial\Omega$ is a 2-D closed contour surrounding the plasma, j_ϕ is the toroidal plasma current density, B_t and B_n are the tangential and normal components to the integral calculation path, and finally $\xi_i = \xi_i(r, z)$ and $\chi_i = \chi_i(r, z)$ are suitable geometric functions linked through the Grad–Shafranov equation. In particular, the first three moments are often employed to estimate the total plasma current I_p and the position (R_p, Z_p) of the plasma centroid inside the vacuum chamber [10]

$$q_0 = \int_\Omega j_\phi d\Omega = I_p \tag{2}$$

$$q_1 = \int_\Omega z \cdot j_\phi d\Omega = Z_p \cdot I_p \tag{3}$$

$$q_2 = \int_\Omega r^2 \cdot j_\phi d\Omega = R_p^2 \cdot I_p. \tag{4}$$

According to (1), the plasma moments are conveniently computed in terms of magnetic measurements surrounding the plasma: since these integral calculations can be approximated by using a finite set of sensor measurements and suitable weighting coefficients, these three moment values are actually obtained as their estimation $\widehat{q_0}$, $\widehat{q_1}$, and $\widehat{q_2}$.

The initial plasma model (first block in Fig. 2) is a filamentary model of fixed cardinality N_e that takes the magnetic measurements $\mathbf{m}$ and the active coil currents $\mathbf{i_s}$ as input to provide *a first guess plasma* that matches the first three low-order moments.

Generally speaking, a filamentary model is defined by a triple $\{\mathbf{r}_e, \mathbf{z}_e, \mathbf{i}_e\}$ of radial and vertical positions of the filaments, $(\mathbf{r}_e(i) = r_i, \mathbf{z}_e(i) = z_i)$, and value of the filament current $\mathbf{i}_e(i)$, $i = 1, \ldots, N_e$: this translates into a solution characterized by $3N_e$ unknowns. In a more simplified fashion, the filament position can be chosen *a priori* (as done in [11]), so that the problem boils down to the current distribution computation (N_e unknowns).

In this spirit, to approximate the first three moments (2)–(4) with a preliminary current distribution and reduce the number of unknowns, a fixed position filamentary model with three degrees of freedom (d.o.f.) is employed to fit a sinusoidal current distribution of the kind

$$\mathbf{i}_{e0}(i) = I_0 + \underbrace{I_c \cos\theta_i}_{I_{\cos}} + \underbrace{I_s \sin\theta_i}_{I_{\sin}} \tag{5}$$

where I_0 is a current bias, and the $I_{\cos}$ and $I_{\sin}$ are sinusoidal contributions, with respect to the ith filament position in (r_i, z_i). The filaments are symmetrically distributed on the ellipse with semiaxes a and b centered in (r_0, z_0) [taken for the ITER geometry as $(6.2, 0.5)$]

$$r_i = r_0 + a\cos\theta_i$$
$$z_i = z_0 + b\sin\theta_i$$

with $\theta_i = (2\pi i / N_e)$, N_e is a multiple of 4 to ensure symmetry with respect to both r and z, and $a, b \in \mathbb{R}_+$ [blue curve in Fig. 3(a)].

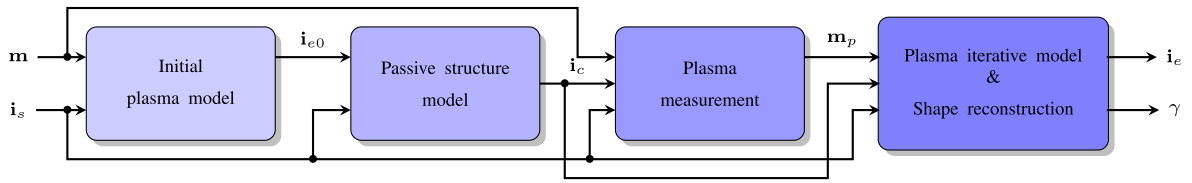

Fig. 2. Schematic of the procedure. An initial filamentary plasma model is employed to estimate the dynamics of the passive structures; this contribution is then filtered from the measurements to allow refinement of the plasma model and identification of the plasma shape and boundary.

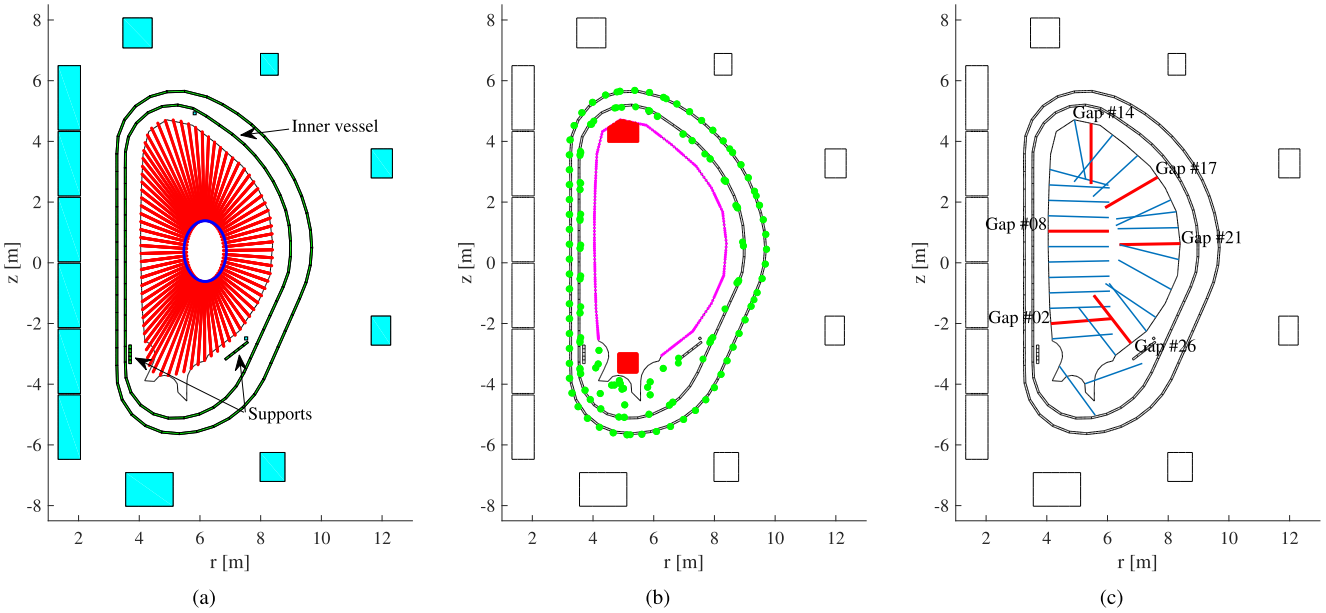

Fig. 3. Geometric elements of the identification procedure on a machine poloidal cross section. (a) Plasma model and machine conducting elements: the first guess plasma filamentary model (with three d.o.f.) is shown in blue dots; the plasma filament positions are then iteratively sought along the rays highlighted in red. The active coils are shown in cyan, while the passive structure elements are depicted in green. (b) Last closed surface identification relies on the x-point and limiter point search in, respectively, the red areas at the bottom and top part of the machine, and the magenta contour along the firstwall. The magnetic sensors surrounding the plasma and allowing for the equilibrium and dynamics reconstructions are also shown, as green dots. (c) Shape descriptors are provided in terms of gaps as plasma-firstwall distances along a set of gaplines, here represented as blue lines; the six reference gaps chosen to check the quality of the reconstruction in the validation section are labeled and highlighted as red thick lines.

Given these assumptions the discrete versions of (2)–(4) based on such model yield

$$\widehat{q_0} = \sum_{i=1}^{N_e} (I_0 + I_c \cos\theta_i + I_s \sin\theta_i) = N_e I_0$$

$$\widehat{q_1} = \sum_{i=1}^{N_e} (z_0 + b\sin\theta_i)(I_0 + I_c \cos\theta_i + I_s \sin\theta_i)$$

$$= z_0 \; N_e I_0 + b I_s \frac{N_e}{2}$$

$$\widehat{q_2} = \sum_{i=1}^{N_e} (r_0 + a\cos\theta_i)^2 (I_0 + I_c \cos\theta_i + I_s \sin\theta_i)$$

$$= r_0^2 \; N_e I_0 + a^2 I_0 \frac{N_e}{2} + a r_0 \; I_c N_e.$$

A linear problem follows where the unknown is the filamentary model triple $\{I_0, I_s, I_c\}$ and the input data are the low-order moment triple $\{\widehat{q_0}, \widehat{q_1}, \widehat{q_2}\}$, with chosen parameters $\{r_0, a, b, N_e\}$: from the simple sparse structure of the moment expression, it follows that:

$$\begin{bmatrix} I_0 \\ I_s \\ I_c \end{bmatrix} = \begin{bmatrix} N_e & 0 & 0 \\ z_0 N_e & \frac{b}{2} N_e & 0 \\ r_0^2 N_e + \frac{a^2}{2} N_e & 0 & a r_0 N_e \end{bmatrix}^{-1} \begin{bmatrix} \widehat{q_0} \\ \widehat{q_1} \\ \widehat{q_2} \end{bmatrix}$$

and hence, the $\mathbf{i}_e(i)$ are obtained through (5).

D. Passive Structure Dynamic Modeling

Once the current sources are known (active circuits, $\mathbf{i}_s$ and plasma filaments, as an initial guess $\mathbf{i}_{e0}$) it is important to understand how these interact with the metallic vessels that contain the plasma and the massive elements that constitute the supporting mechanical structure. In this respect, the estimation of the currents that passively appear and flow in the structures due to the dynamics of the system is a key issue, in that they may be misinterpreted by the external measurements as a contribution of the plasma itself. From a control point of view, this can lead to a wrong comprehension over the role of the passive stabilization that counteracts plasma instabilities while the active control fields penetrate the vessel shielding.

The problem can be cast as follows. The derivative of the magnetic flux Ψ_c linked to the elements of the passive structure, is related to the currents $\mathbf{i}_c$ flowing in the same elements through the diagonal resistance matrix $\mathbf{R}_c$

$$\dot{\Psi}_c + \mathbf{R}_c \mathbf{i}_c = 0$$

and it can be expressed in terms of the current variations as

$$(\mathbf{M}_{cc}\dot{\mathbf{i}}_c + \mathbf{M}_{cp}\dot{\mathbf{i}}_{e0} + \mathbf{M}_{cs}\dot{\mathbf{i}}_s) + \mathbf{R}_c \mathbf{i}_c = 0$$

where $\mathbf{M}_{cc}$, $\mathbf{M}_{cp}$, and $\mathbf{M}_{cs}$ are the mutual inductance matrices of the elements of the passive structure, respectively, with themselves, with the plasma, and with the active coils.

By taking the quantity Ψ_c as the system state variable, plasma and active currents as the input, and $\mathbf{i}_c$ as an output of interest, the system dynamics of the plasma and the surrounding structures can be recast in state-space form as

$$\dot{\Psi}_c = \underbrace{-\mathbf{R}_c\mathbf{M}_{cc}^{-1}}_{\mathbf{A}}\Psi_c + \underbrace{\mathbf{R}_c\mathbf{M}_{cc}^{-1}\mathbf{M}_{cp}}_{\mathbf{B}_p}\mathbf{i}_{e0} + \underbrace{\mathbf{R}_c\mathbf{M}_{cc}^{-1}\mathbf{M}_{cs}}_{\mathbf{B}_s}\mathbf{i}_s$$

$$\mathbf{i}_c = \underbrace{\mathbf{M}_{cc}^{-1}}_{\mathbf{C}}\Psi_c \underbrace{-\mathbf{M}_{cc}^{-1}\mathbf{M}_{cp}}_{\mathbf{D}_p}\mathbf{i}_{e0} \underbrace{-\mathbf{M}_{cc}^{-1}\mathbf{M}_{cs}}_{\mathbf{D}_s}\mathbf{i}_s.$$

With the definitions

$$\mathbf{A} = -\mathbf{R}_c\mathbf{M}_{cc}^{-1} \quad \mathbf{B}_p = \mathbf{R}_c\mathbf{M}_{cc}^{-1}\mathbf{M}_{cp} \quad \mathbf{B}_s = \mathbf{R}_c\mathbf{M}_{cc}^{-1}\mathbf{M}_{cs}$$
$$\mathbf{C} = \mathbf{M}_{cc}^{-1} \quad \mathbf{D}_p = -\mathbf{M}_{cc}^{-1}\mathbf{M}_{cp} \quad \mathbf{D}_s = -\mathbf{M}_{cc}^{-1}\mathbf{M}_{cs}.$$

it follows that:

$$\begin{cases} \dot{\Psi}_c = \mathbf{A}\Psi_c + \begin{bmatrix} \mathbf{B}_p & \mathbf{B}_s \end{bmatrix} \begin{bmatrix} \mathbf{i}_{e0} \\ \mathbf{i}_s \end{bmatrix} \\ \mathbf{i}_c = \mathbf{C}\Psi_c + \begin{bmatrix} \mathbf{D}_p & \mathbf{D}_s \end{bmatrix} \begin{bmatrix} \mathbf{i}_{e0} \\ \mathbf{i}_s \end{bmatrix}. \end{cases} \tag{6}$$

In the specific case of the chosen geometry, $\mathbf{i}_c$ and Ψ_c are column vectors of size $n_c = 110$, $\mathbf{i}_{e0}$ has dimension $n_e = 100$, and $\mathbf{i}_s$ is composed of $n_s = 14$ elements. Hence, $\mathbf{A}, \mathbf{C} \in \mathbb{R}^{n_c \times n_c}$, $\mathbf{B}, \mathbf{D} \in \mathbb{R}^{n_c \times (n_e+n_s)}$.

Starting from the physical derivation described so far, system $\Sigma = (\mathbf{A}, \mathbf{B}, \mathbf{C}, \mathbf{D})$ clearly represents a passive system: indeed, from a control system point of view, the state matrix $\mathbf{A}$ presents stable eigenvalues [Fig. 4(a)] with a dynamic response vanishing to zero. Moreover, Σ is both fully observable ($\mathbf{C}$ is full rank) and controllable and it is thus a minimal realization of its transfer function: hence, it is said to be passive according to the characterization provided by the Kalman–Yakubovich–Popov lemma (see the formulation in [12]). The modal analysis of the state matrix also reveals interesting patterns in the generation of eddy currents on the passive structure elements as shown in Fig. 4(b): these patterns are related to the induced currents due to vertical and radial displacements of the plasma column inside the vacuum vessel (Modes #1–#2) and to higher order patterns as the mode index increases (e.g., Modes #4–#5–#19–#20).

Remark 1: It has to be noted that the equations leading to model (6) could be also written for a different choice of the state variables and, in particular, a more refined plasma discretized model could be adopted in order to obtain a more accurate dynamic behavior description. Nonetheless, the choice of the (simple) model $\mathbf{i}_{e0}$ is motivated by observing that Σ aims at providing a sufficiently good estimate of the

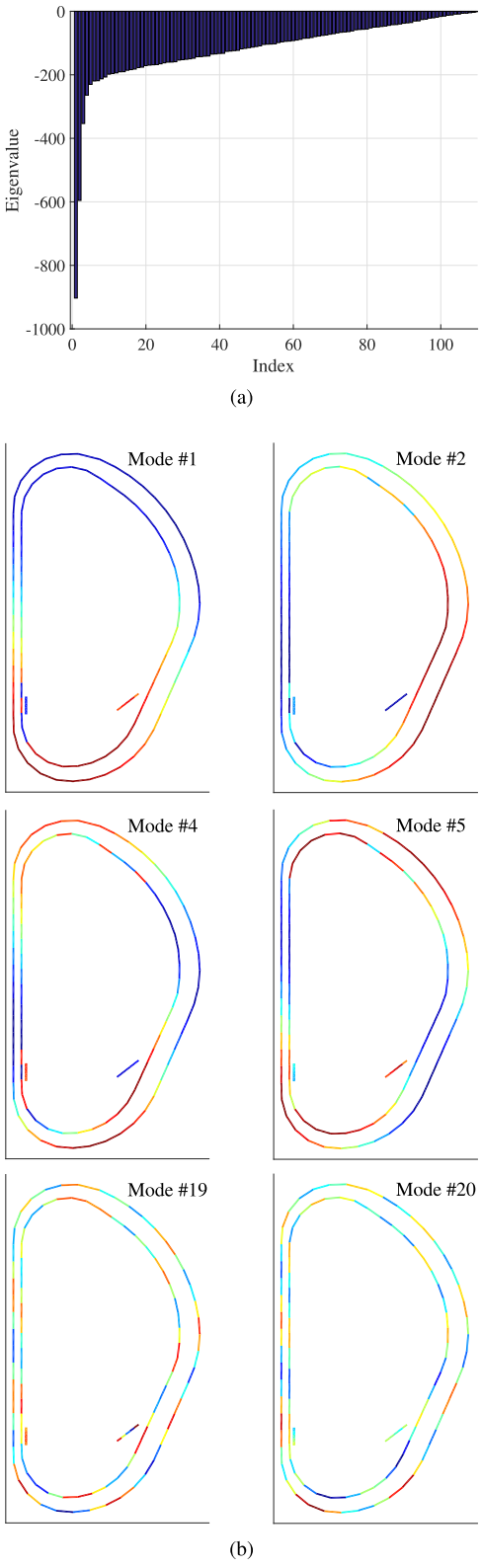

Fig. 4. Modal analysis of model Σ. (a) Eigenvalues of state matrix $\mathbf{A}$. (b) Pattern of modes appearing on the passive structures: red and blue shadings correspond, respectively, to high and low values of the mode (namely, positive/negative eddy currents), while green shading is related to null values.

passive currents $\mathbf{i}_c$. As it will be shown in the validation Section III, this choice reveals to be accurate enough for the purpose of interest.

On the other hand, while in this paper the passive elements of the vessels and the plasma-facing components are discretized according to a geometric approach, the models of these and other structures are often obtained from FE procedures. These approaches result in high-dimensional descriptions that require model reduction techniques to be applied so as to provide a manageable system Σ [13]. □

E. Plasma Measurements

The dynamic description of the passive elements currents $\mathbf{i}_c$ allows to estimate the actual contribution of the plasma to the magnetic measurements. Actually, the magnetic measurements $\mathbf{m}$ (of cardinality n_m) are given by the superimposed effects of the plasma current, the active coil currents, and the passive structure currents, respectively, $\mathbf{m}_p$, $\mathbf{m}_s$, and $\mathbf{m}_c$

$$\mathbf{m} = \mathbf{m}_p + \mathbf{m}_s + \mathbf{m}_c$$

which is an instantaneous relation that reduces to the following in the case that the dynamic effects are vanished:

$$\mathbf{m} = \mathbf{m}_p + \mathbf{m}_s.$$

Then, since the active coil currents $\mathbf{i}_s$ are known and the passive structure currents $\mathbf{i}_c$ can be obtained as the output of system (6), through employment of Green's function that relates the magnetic flux/field in a specific location with the currents that generate it [14], in the more general dynamic case it is

$$\mathbf{m}_p = \mathbf{m} - \mathbf{G}_{\mathrm{ms}}\mathbf{i}_s - \mathbf{G}_{\mathrm{mc}}\mathbf{i}_c$$

where $\mathbf{G}_{\mathrm{ms}} \in \mathbb{R}^{n_m \times n_s}$ and $\mathbf{G}_{\mathrm{mc}} \in \mathbb{R}^{n_m \times n_c}$ are the Green matrices that provide the magnetic sensor measurements with respect to the active coils and the passive positions. In this way, the measurement vector $\mathbf{m}_p$ contains the information related only to the plasma current contribution, as schematically (and logically) shown in the third block in Fig. 2.

Remark 2: In this respect, it is interesting to highlight the fact that the simplified plasma model with three d.o.f. (5) is sufficient to estimate the passive structure currents $\mathbf{i}_c$ but not optimal to carry out the identification of the boundary of the plasma and its shape, for which a more complex model with higher d.o.f. is needed, as developed in the following section. □

F. Plasma Iterative Model

The fourth block in Fig. 2 takes the active coil currents $\mathbf{i}_s$ and the measurements $\mathbf{m}_p$ due to the plasma only in input and provides the plasma shape descriptions γ: these can be given in terms of plasma-firstwall distances along predefined lines, i.e., gaps, the position of the magnetic x-points, and/or other flux information outside the plasma.

The implemented procedure is based on an Iterative Axisymmetric Identification Algorithm that adaptively allocates a set of plasma equivalent currents $\mathbf{i}_e$ to obtain the best estimate of the plasma contour, and it was initially presented in [8].

The approach adopted to obtain this model is based on a static best fitting of the available magnetic measurements to compute the model parameters. This calculation involves computation of the eigenvalues of a map between the equivalent currents $\mathbf{i}_e$ and the measurement contribution due to the plasma $\mathbf{m}_p$: the larger the eigenvalues, the stronger is the relation between the two sets of quantities. The cardinality N_e of the filamentary model and the positions of the equivalent current set are d.o.f. of the inverse identification problem and they must be *a priori* assigned [15]. The input quantities (known terms) of the identification problem are a set of n_m magnetic measurements (flux loops and pickup probes) placed inside and outside the vacuum vessel [see Fig. 3(b)].

1) Least Square Solution: Then, for a given arrangement, the values of the equivalent currents $\mathbf{i}_e$ can be calculated as the solution of the following inverse problem:

$$\mathbf{m}_p = \mathbf{G}_{\mathrm{mp}}\mathbf{i}_e$$

where $\mathbf{m}_p$ represents the contribution of plasma to the measurements $\mathbf{m}$: unfortunately $\mathbf{G}_{\mathrm{mp}}$ is usually not-invertible. This is due to the fact that the chosen measurements are not linearly independent, which translates into a rank-deficient matrix or to a number of unknowns different from the number of measurement data, i.e., underdetermined/overdetermined problems.

Therefore, we cast this problem into an optimization framework: in other words, starting from the observational data $\mathbf{m}_p$, we want to find the best distribution $\widehat{\mathbf{i}}_e$ that allows to approximate (and no longer to exactly match) the measurements $\mathbf{m}_p$

$$\widehat{\mathbf{i}}_e = \min_{\mathbf{i}_e} \|\mathbf{G}_{\mathrm{mp}}\mathbf{i}_e - \mathbf{m}_p\|_2 \tag{7}$$

where $\|\mathbf{G}_{\mathrm{mp}}\mathbf{i}_e - \mathbf{m}_p\|_2$ represents a chosen (scalar) objective function ϕ (in this case the approximation error).

This problem can be solved by differentiating the objective function ϕ with respect to $\mathbf{i}_e$

$$\nabla_{\mathbf{i}_e}\|\mathbf{G}_{\mathrm{mp}}\mathbf{i}_e - \mathbf{m}_p\|_2^2 = 2\mathbf{G}_{\mathrm{mp}}^\top\mathbf{G}_{\mathrm{mp}}\mathbf{i}_e - 2\mathbf{G}_{\mathrm{mp}}^\top\mathbf{m}_p.$$

Equalling this to zero leads to the so-called normal equations

$$\mathbf{G}_{\mathrm{mp}}^\top\mathbf{G}_{\mathrm{mp}}\mathbf{i}_e - \mathbf{G}_{\mathrm{mp}}^\top\mathbf{m}_p = 0$$

which have a solution if matrix $\mathbf{G}_{\mathrm{mp}}^\top\mathbf{G}_{\mathrm{mp}}$ is positive definite[1]

$$\widehat{\mathbf{i}}_e = (\mathbf{G}_{\mathrm{mp}}^\top\mathbf{G}_{\mathrm{mp}})^{-1}\mathbf{G}_{\mathrm{mp}}^\top\mathbf{m}_p.$$

2) Regularized Solution: In general, it may happen that (7) is ill-conditioned, the extent of the ill-conditioning strongly depending both on the probe locations (a crucial issue in the design of new machines) and on the arrangement selected for the equivalent currents. In this case, the numerical solution of (7) requires a regularization method to obtain a unique regular solution approximating the desired vector $\mathbf{m}_p$ [16]. A singular values decomposition (SVD) technique is usually adopted to approximate the ill-conditioned matrix $\mathbf{G}_{\mathrm{mp}}$ with a better-conditioned matrix.

[1] This corresponds to the least square solution to the initial problem (7).

It can be assumed a number of current filaments N_e (that now refers to the current set $\mathbf{i}_e$) lower than the number of available measurements n_m, $N_e < n_m$: by computing the SVD of the matrix we obtain

$$\mathbf{G}_{\text{mp}} = \mathbf{U}\,\mathbf{S}\,\mathbf{V}^{\top}$$

being $\mathbf{S} \in \mathbb{R}^{n_m \times N_e}$ the extension of the diagonal matrix of the singular values σ, $k = 1, \ldots, N_e$ of $\mathbf{G}_{\text{mp}}$ padding with zeros the last $(n_m - N_e)$ rows, and $\mathbf{U} \in \mathbb{R}^{n_m \times n_m}$, $\mathbf{V}^{\top} \in \mathbb{R}^{N_e \times N_e}$ orthogonal matrices. The solution vector can be expressed as

$$\widehat{\mathbf{i}}_e = \mathbf{V}\mathbf{S}^{+}\mathbf{U}^{\top}\mathbf{m}_p = \sum_{k=1}^{N_e} \frac{(\mathbf{U}^{\top}\mathbf{m}_p)(k)}{\sigma_k}\mathbf{v}_k \tag{8}$$

where the pseudoinverse of the matrix $\mathbf{S}$ is obtained by replacing the nonzero elements of $\mathbf{S}$ with their inverse and $\mathbf{v}_k$ indicates the kth column of $\mathbf{V}$. Scalarly, the iith current results from the following:

$$\widehat{\mathbf{i}}_e(ii) = \underbrace{\begin{bmatrix}\mathbf{V}(ii,1) & \ldots & \mathbf{V}(ii,N_e)\end{bmatrix}}_{\mathbf{V}\text{'s } ii\text{-th row}} \begin{bmatrix} \frac{(\mathbf{U}^{\top}\mathbf{m}_p)(1)}{\sigma_1} \\ \ldots \\ \frac{(\mathbf{U}^{\top}\mathbf{m}_p)(N_e)}{\sigma_{N_e}} \end{bmatrix}$$

where $(\mathbf{U}^{\top}\mathbf{m}_p)(k)$ indicates the kth element of the vector $\mathbf{U}^{\top}\mathbf{m}_p$.

By operating an SVD truncation at the rth order ($r < N_e$), meaning that we are retaining only the r larger singular values, it follows that:

$$\widehat{\mathbf{i}}_e^{(r)} = \mathbf{V}\mathbf{S}_{\mathbf{r}}{}^{+}\mathbf{U}^{\top}\mathbf{m}_p = \sum_{k=1}^{r} \frac{(\mathbf{U}^{\top}\mathbf{m}_p)(i)}{\sigma_k}\mathbf{v}_k$$

where in $\mathbf{S}_{\mathbf{r}}$ the neglected σ_k's are set to zero. Equivalently

$$\widehat{\mathbf{i}}_e^{(r)}(ii) = \begin{bmatrix}\mathbf{V}(ii,1) & \ldots & \mathbf{V}(ii,r)\end{bmatrix} \begin{bmatrix} \frac{(\mathbf{U}^{\top}\mathbf{m}_p)(1)}{\sigma_1} \\ \ldots \\ \frac{(\mathbf{U}^{\top}\mathbf{m}_p)(r)}{\sigma_r} \end{bmatrix}.$$

3) Iterative Procedure: Unfortunately, the matrix $\mathbf{G}_{\text{mp}}$ needs to be computed online since the choice of the "active" filaments occurs in real-time.

Differently from the initial plasma model $\mathbf{i}_{e0}$, which has a fixed position (discrete) ring structure in the poloidal coordinate, the active filaments of $\mathbf{i}_e$ are free to move independently along a set of rays that go from the inside of the vacuum vessel toward the first wall [red lines in Fig. 3(a)]. Along these lines (current rays), filamentary currents are selected according to the iterative procedure described as follows.

1) First, a set of equivalent currents is placed at the beginning of the current rays, well inside the plasma domain, in an area that is basically included in any plasma cross section shape;
2) the current distribution $\mathbf{i}_{\text{ei}}$ on this inner set is computed according to the optimization problem (7).
3) Given this current distribution, a flux map is generated, the value of the boundary flux is determined by comparing the values at the firstwall and in the x-point areas to discern between limiter and diverted configurations [see Fig. 3(b)]
4) A first guess of the plasma boundary is computed.
5) Then, iteratively:
   a) a second set of equivalent currents is placed along the rays, midway between the starting point of the ray and the currently identified boundary (in order to avoid local artifacts induced by the filamentary model, the equivalent currents are in any case kept at a minimum distance from the identified boundary);
   b) the current distribution $\mathbf{i}_{\text{eo}}$ on this outer set is computed together with a new $\mathbf{i}_{\text{ei}}$ according to the optimization problem (7);
   c) a further boundary is computed;
   d) the procedure is iterated.

It can be chosen to have a fixed number of iterations (experimentally we can state that three iterations are sufficient to reconstruct plasmas with edge current distributions), or setting a convergence criterion with reference to some distance measurement between two consecutive iterations (e.g., difference of current distribution or difference of reconstructed shape or error in reconstructing some measurements). In this latter case, an accurate study of the adopted metrics is due.

G. Algorithm Convergence and General Robustness

The convergence of the iterative procedure is guaranteed by the bisection procedure over a finite set of points, used in conjunction with a saturation limit. In principle, an upper bound $\hat{k}_{\text{it}}$ to the number of the iteration is given by the discretization of the lines along which the iterative model is moving (N points) and can be computed as

$$\hat{k}_{\text{it}} = \min k \quad \text{s.t. } 2^k \geq N$$

leading to a maximum of seven iterations in the studied case with $N = 120$. Nonetheless, to ensure the same execution time to every reconstruction instance, a fixed number of iterations appear as a good tradeoff choice to obtain good reconstruction performances. Furthermore, this assumption also limits the effects of oscillatory behaviors that in principle may appear. In practice, though, these were never observed in the experimental validation and $\hat{k}_{\text{it}}$ has been set equal to 3.

The choice has been made not to exploit the variable information (e.g., currents, boundary location) computed at the previous time step of the scenario to guarantee similar convergence properties at any step and avoid the propagation of estimation errors, which would hinder a possible corrective action. Moreover, this enhances the precision (reproducibility) of the algorithm, since it allows the bisection procedure to provide exactly the same output for the same signal input set.

III. Validation

The assessment and validation of the algorithm consider the following:

1) the algorithm convergence and general robustness;
2) capability of reconstruction of the boundary location along a set of poloidal gap distances (distances along gaplines); quantification of the reconstruction error with

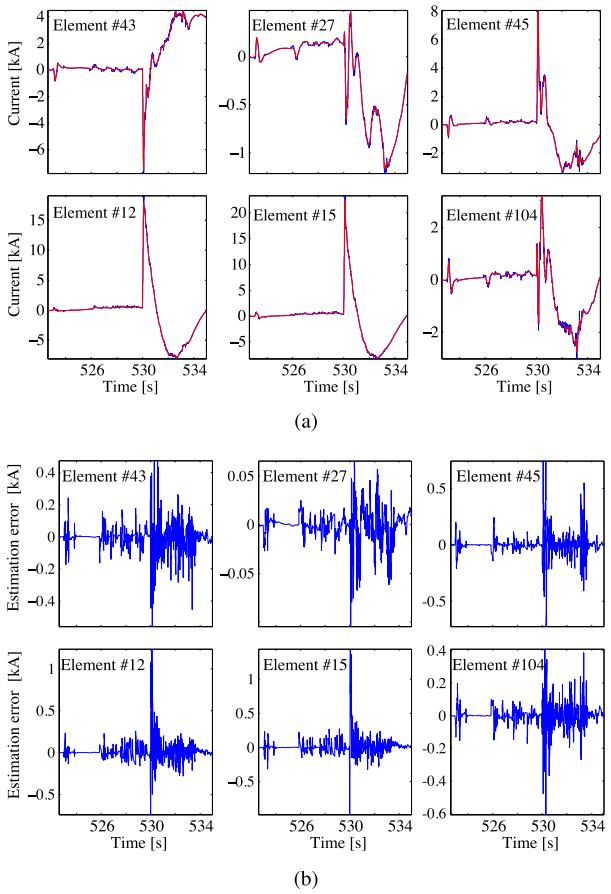

Fig. 5. Eddy current estimation in the passive structure elements. (a) Current values and (b) estimation errors in a subset of elements from the inner vessel (#1–#50) and supports (#101–#110). The estimated quantity (red) is shown against the reference one (blue) obtained from a simulation code.

respect to a simulation code is in the range of ± 1 cm in static conditions (equilibrium reconstruction);

3) robustness to noise in the measurements;
4) capability of estimation of the eddy currents in the passive structures during dynamic events.

The validation of the procedure is carried out with respect to a complete scenario developed with the equilibrium code CREATE-NL (see details in [17]), providing both input waveform references for the active coils and plasma global quantities (β_p, ℓ_i), and output sensor measurements and boundary location. The scenario is constituted by an RU phase at low plasma current (at around 2MA), toward an FT ($I_p = 15$MA), which comprises highly dynamic transitions from low to high energy confinement mode (early phase of FT) and back from high to low (at $t = 530$ s), and then concludes with an RD phase. The timings of the scenario and the three phases are shown in the top panel in Fig. 6, with reference to the plasma current.

To prove the feasibility of the employment of the simplified plasma model (5) for estimation of the passive elements currents, an example of the eddy current reconstruction is provided in Fig. 5: it can be seen that this simple model with three d.o.f. is sufficient to provide accurate reconstruction of the eddy currents with the advantage of being based on a

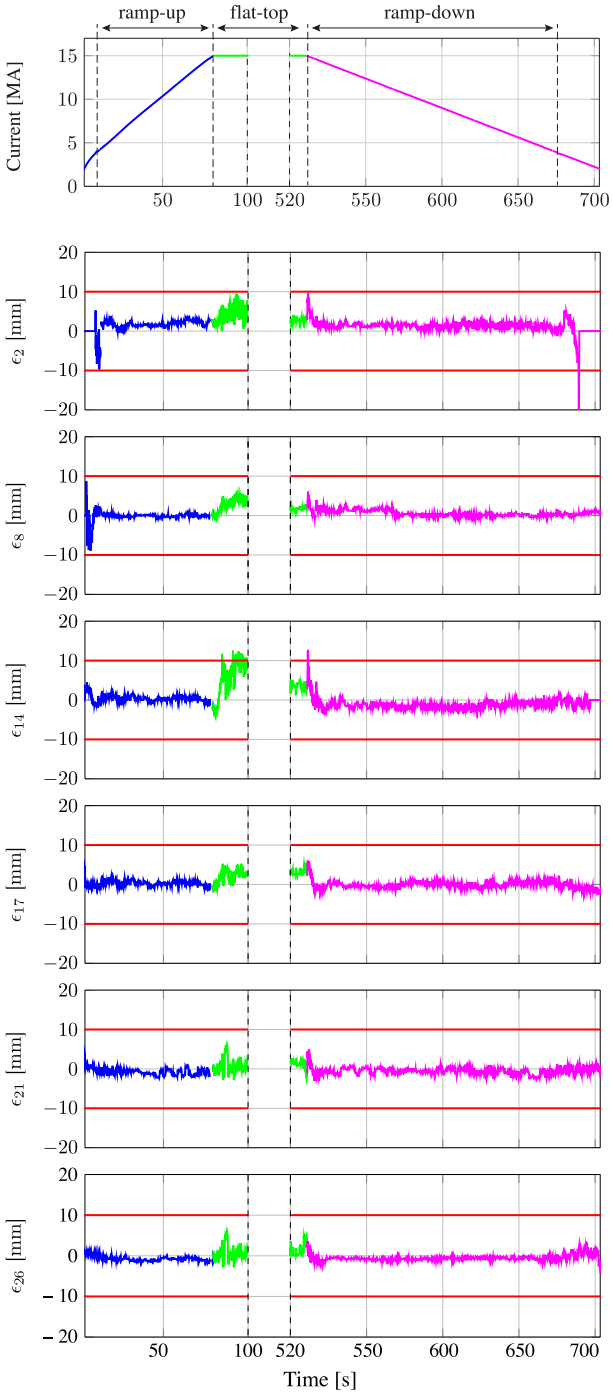

Fig. 6. Time evolution of plasma current and boundary error along the six reference gaplines highlighted in Fig. 3(c).

closed-form solution, also in the presence of high dynamics as at $t = 530$ s (high to low energy confinement transition).

Reconstruction of the plasma boundary is carried out for a complete evolution, and a comparison between the ground-truth (real) boundary of the nonlinear equilibrium code and the reconstructed boundary is shown along the six chosen reference gaplines highlighted in Fig. 3(c). The deviation between the real boundary and the reconstructed one along these six gaps is reported in the six lower panels of Fig. 6: this

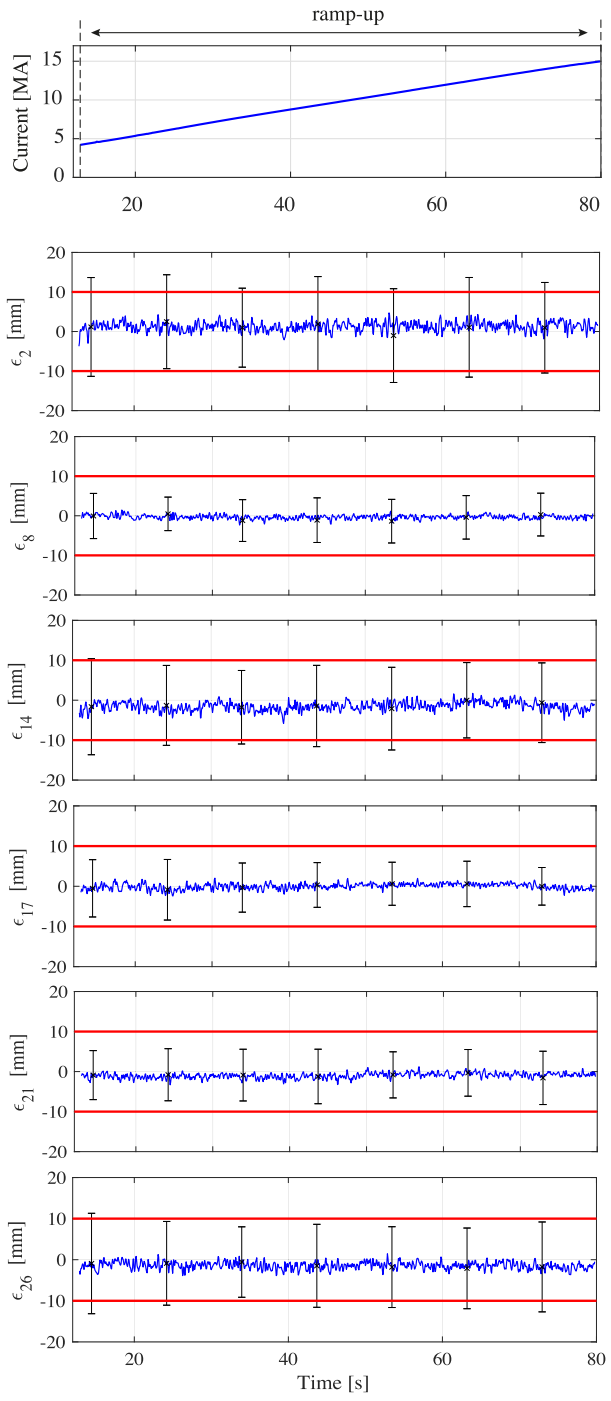

Fig. 7. Time evolution of boundary error during the RU phase along the reference gaplines of Fig. 6 in the presence of measurement noise. The solid line denotes the average error computed in 500 runs with a random distribution of measurement noise, while the error bars denote the standard deviation.

deviation is almost always bounded between ± 10 mm, (thick red lines), with the exception of the early RU and at the end of the RD, where the deviation is bounded between ± 20 mm (dashed lines).

A final observation is due on the algorithm robustness to noise. It is of note that magnetic diagnostic systems in fusion machines can be affected by several sources of errors (from the nonideality of the sensor/measurement chain to the effects of radiation) and, in this sense, an agreed sensor measurement model for the ITER machine considers such total error as proportional to the actual value of the signal. Hence, in a further validation of the algorithm, a Monte Carlo simulation approach has been adopted and for each sensor used in input to the reconstruction procedure, the (noisy) measured signal $\widetilde{\mathbf{m}}$ has been calculated from its actual (ideal) value $\mathbf{m}$ as

$$\widetilde{\mathbf{m}} = (1 + \sigma_r)\mathbf{m}$$

where the measurement noise has a normal distribution with a zero mean and standard deviation σ_r. Specifically, the simulations reported here are run with the in-vessel pickup sensor set and $\sigma_r = 0.7\%$, which reflects a total error target of 0.7% with 95% confidence due to the noise level, as indicated for ITER in-vessel magnetics. The results of this assessment (shown in Fig. 7 for the RU phase) confirm the validity of the approach and the consistence of the boundary reconstruction with the required accuracy, also in the presence of measurement noise.

IV. Conclusion

In this paper, a model-based procedure for reconstruction of the shape in fusion plasmas is developed and discussed. The proposed approach is based on a dynamical model of the eddy currents with an iterative algorithm that solves an inverse optimization problem to converge to a suboptimal filamentary plasma distribution. As validation, the flux map over the cross section of the machine is computed and compared with that provided by an equilibrium code, showing that the reconstruction capability of the procedure is good enough to be considered for real-time employment during the whole scenario.

Acknowledgment

The authors would like to thank Dr. M. Cavinato of Fusion for Energy for the fruitful discussion and support throughout the development of this paper.

References

[1] A. Pironti and M. Walker, "Control of tokamak plasmas: Introduction to a special section," *IEEE Control Syst.*, vol. 25, no. 5, pp. 24–29, Oct. 2005.

[2] M. Ariola and A. Pironti, *Magnetic Control of Tokamak Plasmas* (Advances in Industrial Control). London, U.K.: Springer-Verlag, 2016.

[3] R. Ambrosino, G. De Tommasi, M. Mattei, and A. Pironti, "Model based optimization and estimation of the field map during the breakdown phase in the ITER tokamak," in *Proc. IEEE Conf. Control Appl. (CCA)*, Sep. 2015, pp. 1284–1289.

[4] L. Berzak *et al.*, "Magnetic diagnostics for equilibrium reconstructions in the presence of nonaxisymmetric eddy current distributions in tokamaks (invited)," *Rev. Sci. Instrum.*, vol. 81, no. 10, p. 10E114, 2010.

[5] A. C. Neto *et al.*, "MARTe: A multiplatform real-time framework," *IEEE Trans. Nucl. Sci.*, vol. 57, no. 2, pp. 479–486, Apr. 2010.

[6] J. Doody, B. Lipschultz, R. Granetz, W. Beck, and L. Zhou, "Modeling technique to predict fields, currents, and loads for C-Mod's advanced outer divertor during a disruption with a 2.5-MA plasma current and 9-T toroidal field," *IEEE Trans. Plasma Sci.*, vol. 42, no. 3, pp. 568–572, Mar. 2014.

[7] S. Peruzzo *et al.*, "Integrated procedure for halo current reconstruction in ITER," *IEEE Trans. Plasma Sci.*, vol. 41, no. 1, pp. 257–262, Jan. 2013.

[8] P. Bettini and A. Cenedese, "Iterative axisymmetric identification algorithm (IAIA) for real-time reconstruction of the plasma boundary of ITER," *Fusion Eng. Des.*, vol. 88, nos. 6–8, pp. 1150–1155, 2013.

[9] L. E. Zakharov and V. D. Shafranov, "Equilibrium of a toroidal plasma with noncircular cross section," *Sov. Phys. Tech. Phys.*, vol. 18, no. 2, pp. 151–156, Aug. 1973.
[10] B. P. van Milligen, "Exact relations between multipole moments of the flux and moments of the toroidal current density in tokamaks," *Nucl. Fusion*, vol. 30, no. 1, p. 157, 1990.
[11] A. Cenedese, F. Sartori, and M. Macuglia, "Development of fixed-position filamentary plasma model based on the current moment description," *IEE Proc.-Sci., Meas. Technol.*, vol. 151, no. 6, pp. 484–487, Nov. 2004.
[12] E. Kaszkurewicz and A. Bhaya, *Matrix Diagonal Stability in Systems and Computation*. Boston, MA, USA: Birkhäuser, 2000.
[13] A. Cenedese, M. Fagherazzi, and P. Bettini, "A novel application of selective modal analysis to large-scale electromagnetic devices," *IEEE Trans. Magn.*, vol. 52, no. 3, Mar. 2016, Art. no. 7203304.
[14] D. Duffy, *Green's Functions With Applications* (Applied Mathematics). Boca Raton, FL, USA: CRC Press, 2001.
[15] P. Bettini, M. Cavinato, and F. Trevisan, "Dynamic identification of plasma magnetic contour in fusion machines," *Nucl. Fusion*, vol. 45, no. 1, p. 1, 2005.
[16] C. Lawson and R. Hanson, *Solving Least Squares Problems* (Classics in Applied Mathematics). Philadelphia, PA, USA, SIAM, 1995.
[17] R. Albanese, R. Ambrosino, and M. Mattei, "CREATE-NL+: A robust control-oriented free boundary dynamic plasma equilibrium solver," *Fusion Eng. Des.*, vols. 96–97, pp. 664–667, Oct. 2015.

Angelo Cenedese (M'11) received the M.S. and Ph.D. degrees from the University of Padua, Padua, Italy, in 1999 and 2004, respectively.

He has held several visiting positions at the International Universities and Research Centers: the United Kingdom Atomic Energy Authority-Joint European Torus Laboratories, the Culham Research Center, Abingdon, U.K., from 2002 to 2004, the Japan Atomic Energy Research Institute, Naka, Japan, in 2000, General Atomics, San Diego, CA, USA, in 2004, the UCLA Vision Lab, San Diego, CA, USA, in 2010, and the Fusion for Energy European Agency, Barcelona, Spain, in 2014. He is currently an Associate Professor with the Department of Information Engineering, University of Padua. He has authored more than 120 papers and holds three patents. His current research interests include system modeling, control theory and its applications, fusion devices, sensor and actuator networks, and multiagent systems.

Dr. Cenedese is a member of the Center for Research on Fusion, University of Padua and a Research Associate of the CNR-IEIIT.

Paolo Bettini was born in Venice, Italy, in 1969. He received the master's and Ph.D. degrees in electrical engineering from the University of Padua, Padua, Italy, in 1994 and 1998, respectively.

From 2005 to 2009, he was an Associate Professor of electrical science and electromagnetic compatibility with the University of Udine, Udine, Italy. Since 2009, he has been an Associate Professor of electrical science and thermonuclear fusion with the University of Padua. He has authored more than 110 indexed scientific publications on several topics concerning the computation of electromagnetic fields and the magnetic confinement fusion.

Matteo Bonotto received the master's degree in electric engineering from the University of Padua, Padua, Italy, where he is currently pursuing the Ph.D. degree in fusion science and engineering with RFX Consortium.

His current research interests include the study of resistive wall modes instabilities in full 3-D geometry of present and future fusion devices in the view of control. He has been involved in model order reduction techniques, real-time identification of plasma boundary in fusion reactors for control purpose, with a focus on the numerical solution of Grad–Shafranov problem using finite element method.